Applied Acoustics 105 (2016) 93–98

Contents lists available at ScienceDirect

Applied Acoustics

journal homepage: www.elsevier.com/locate/apacoust

Technical Note

Characterization of the road surfaces in real time

David Ibarra [a,*], Ricardo Ramírez-Mendoza [a], Saúl Ibarra [b]

[a] Tecnológico de Monterrey, Escuela de Ingeniería y Ciencias, Campus Mexico City, Calle del Puente 222, Ejidos de Huipulco, Tlalpan 14380 Mexico D.F, Mexico
[b] Dragon Laboratory, Calle Cedros Lt. 51 Mz. 11, Paseos de Xhosda, San Juan del Rio 76808, Queretaro, Mexico

ARTICLE INFO

Article history:
Received 31 July 2015
Received in revised form 7 October 2015
Accepted 23 October 2015

Keywords:
Data acquisition
Ground impedance
Road surfaces

ABSTRACT

The main factor in the propagation of traffic noise is the road surface, where the vehicles generate noise due to the contact between tire and pavement, in addition to the noise produced by the engine.

The aim of this work is to obtain the parameters of ground surfaces in real time at different speeds by using an on-board data acquisition system. The system is based on two small microphones with flat response frequency, a small directional speaker, audio interface and a laptop for signal processing.

The contribution of this system is to know, in real time, the physical parameters of ground surface measured at different speeds, minimizing the influence of aerodynamic noise. The low cost and its portability make the system to be a very useful tool for noise predictions in outdoors propagation and could be used as a complement instrument in noise mapping.

The acoustic impedance was measured by the method recommended by the ANSI S1.18 standard, but with some adjustments. This method consists of measuring the sound level difference from two microphones close to the surface, and calculating the level difference according to an impedance model of the ground.

1. Introduction

The effect of the surface is the most influential factor in sound propagation. When noise propagates from the source to the receiver on a reflective surface, the direct and the reflected signals interfere. If the surface has finite impedance, the reflected part interferes with the direct field, allowing a significant reduction of the original noise if the reflective conditions are adjusted properly. These conditions can be modeled either as a local reaction or an extended reaction [1]. The local reaction condition for noise propagation outdoors is very simple, but valid only on a limited range of frequencies. For the study of surfaces that enable the noise transmission inside themselves, the simplest model was developed by Delany and Bazley [2]. It expresses the impedance of the material and its propagation constants based on empirical relationships that depend only on flow resistivity. In this work we show the results obtained using models for one to four parameters.

We aimed to work with an analytical approach allowing us a rough prediction of the noise produced by a source spreading on a ground surface. The attenuation depends on frequency, propagation distance, angle of incidence and geometric configuration of sources and sensors.

For measuring the ground impedance *in-situ*, 'impulse-techni ques' are the best choice, since they make it possible to remove unwanted reflections from the recorded signal. Some experiments have used spark-sources, gunshots, recorded pulses and tone-bursts [3]. However, measuring impulse-responses indirectly using e.g. pseudo-random MLS-sequences [4], has proved to be superior, due to the fact that they are perfectly reproducible, have a high dynamic range and can be applied in noisy environments. Time-windowing, subtraction of free-field signals or other techniques (e.g. cepstral deconvolution) can remove unwanted signals [5].

2. Theoretical model

Let us consider a point source and receiver at heights h_s and h_r, respectively, over a flat surface, separated a lateral distance R, Fig. 1. Let R_1 and R_2 be the source–receiver distance for the real and image sources, respectively, and θ the incidence angle of sound on the surface.

The sound pressure at the receiver is the sum of the direct signal, which comes from the real source, plus the reflected signal from the ground, which is assumed to come from the image source. If a plane wave model is applied, the sound pressure at the receiver should be $p = p_d + R_p\, p_r$, where p_d and p_r are the direct and reflected contributions, respectively, and R_p is the plane wave reflection coefficient, given by [1]

* Corresponding author. Tel.: +52 81 5483 2020.
E-mail address: david.ibarra@itesm.mx (D. Ibarra).

http://dx.doi.org/10.1016/j.apacoust.2015.10.023
0003-682X/

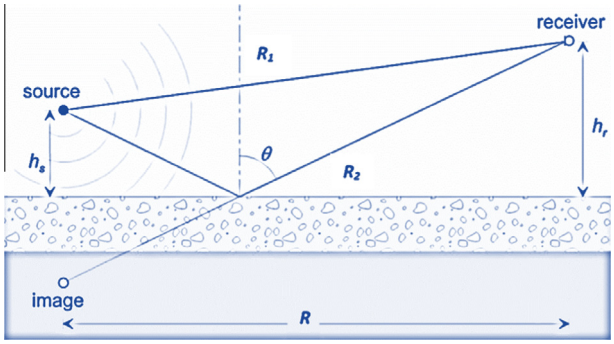

Fig. 1. Geometry for spherical waves propagating on the ground.

$$R_p = \frac{Z_s cos\theta_0 - Z_0}{Z_s cos\theta_0 + Z_0} \tag{1}$$

where Z_s is the surface impedance of the ground, Z_0 is the impedance of the air, θ_s is the transmission angle on the ground, but a spherical wave model must be taken into account. For such a model, Attenborough [5] shows that the sound pressure at the receiver is

$$p(x,y,z) = \frac{e^{jk_0R_1}}{4\pi R_1} + Q\frac{e^{jk_0R_2}}{4\pi R_2}, \tag{2}$$

where

$$Q = R_p(\theta) + [1 - R_p(\theta)]F(w), \tag{3}$$

is the spherical wave reflection coefficient on the ground. Therefore, the spherical wave reflection coefficient is the sum of the plane wave reflection coefficient plus a second term named the ground wave, which depends on the complex function $F(w)$, the so-called boundary loss factor, defined as [6]

$$F(w) = 1 + j\sqrt{\pi}we^{-w^2}erfc(-jw), \tag{4}$$

Erfc being the complementary error function. The complex variable w, in Eq. (4), also known as numerical distance, is

$$w = \frac{1+j}{2}\sqrt{k_0R_2}\left(\frac{Z_0}{Z_s} + cos\theta\right), \tag{5}$$

w is the numerical distance [7,8].

According to this model, the ground attenuation will be [9,10]

$$\Delta L = 20log_{10}\left[\left|1 + Q\frac{R_1}{R_2}e^{jk_0(R_2-R_1)}\right|\right], \tag{6}$$

Thus, a ground impedance model is required to calculate the effect of this boundary in the sound field. Each of the ground layers can be characterized by impedance models of one, two, three or four parameters.

Let us consider a plane wave incident on a surface with angle θ_0, characterized by acoustic impedance Z_s and propagation constant k_s Fig. 2.

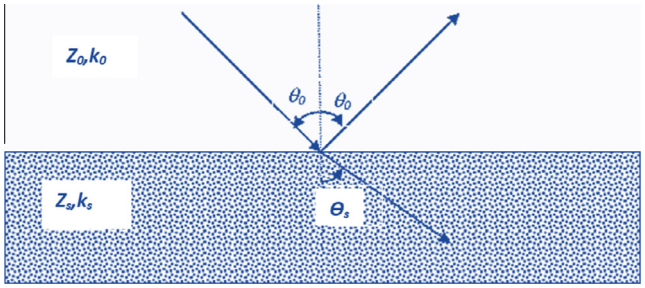

Fig. 2. A plane wave incident on a homogeneous medium.

The impedance model, Z_s, is established for the ground. In this case, a homogeneous locally reacting ground is assumed with normalized acoustic impedance given by the Delany–Bazley equation for one parameter model [2]

$$z_s = (1 + 0.0571E^{-0.754} + j0.087E^{-0.732}), \tag{7}$$

where $E = \rho_0 f/\sigma$, ρ_0 is the air density and σ is the flow resistivity and f the frequency.

This model, which depends on just one parameter (the flow resistivity) has been adopted in some works for calculating the excess attenuation of grounds [11–13].

There is evidence that the one parameter model tends to overestimate the attenuation within a porous material with a high flow resistivity. Attenborough [5] proposed a two parameter model, which includes an exponential change of porosity with depth. This model, also assumed by the ANSI S1.18 [14] standard, proposes

$$Z_s = Z_0\left\{\frac{1}{\sqrt{\pi\gamma\rho_0}}\sqrt{\frac{\sigma_e}{f}} + j\left[\frac{1}{\sqrt{\pi\gamma\rho_0}}\sqrt{\frac{\sigma_e}{f}} + \frac{c_0\alpha_e}{8\pi\gamma f}\right]\right\}, \tag{8}$$

where $\gamma = 1.4$ for an ideal gas, σ_e is the effective flow resistivity of the ground, and α_e (in 1/m) represents the effective rate of porosity change with depth.

Attenborough et al. [15] describe the phenomenological model of three parameters (also named the Zwickker and Kosten model), based on the equation

$$Z_s = \frac{Z_0}{\phi}\left(T + \frac{j\phi\sigma}{\rho_0\omega}\right)^{1/2}, \tag{9}$$

where ϕ is the porosity, T is the tortuosity and σ is the flow resistivity. This model assumes adiabatic conditions in the pores. Other authors proposed a modified model, also called Hamet model [15], more appropriate for porous asphalt. Another three parameter impedance model is the Wilson model [15].

The four parameter impedance model recommended by ANSI S1.18 [14] is

$$Z_s = Z_0\frac{\rho_s(\omega)}{k_s(\omega)}, \tag{10}$$

where

$$\rho_s(\omega) = \left(\frac{4}{3}\frac{T}{\phi} + j\frac{4s_p^2\sigma}{\omega\rho_0}\right), \tag{11}$$

$$k_s^2(\omega) = \gamma\phi\left[\left(\frac{4}{3} - \frac{\gamma-1}{\gamma}N_{pr}\right)\frac{T}{\phi} + j\frac{4s_p^2\sigma}{\omega\rho_0}\right], \tag{12}$$

and γ is the specific heat ratio of air, N_{pr} the Prandtl number, σ the dc component of the flow resistivity, ϕ the ground porosity, T the tortuosity, and S_P a shape factor. Assuming that $T = \phi^{-n}$, where n depends on the shape of the grains.

3. System and equipment

The experimental measurements were performed along several avenues, in the south part of Mexico City. The following equipment was used: two small omnidirectional microphones, with frequency response of 20–20,000 Hz; small directional speaker with frequency response of full range; audio interface of 2 channels, with sampling frequency of 96 kHz; a laptop and software for signal processing.

The two microphones were mounted on a support and a base of wood for the source, and were installed in a sports utility vehicle as shown in Fig. 3. The microphones were placed at different heights from the soil: 0.06 m and 0.165 m; the source was at a height of 0.165 m, and the distance between microphones and speaker was

Fig. 3. Experimental setup.

0.4 m. The geometry setup recommended by ANSI S1 standard was not possible to adopt due to the conditions and the portability. Fig. 3 shows the experimental setup.

4. Ground impedance measurements

The purpose of this work was to measure the sound level difference of two microphones, positioned at heights *Ht* (height of top microphone) and *Hb* (height of bottom microphone) when a loudspeaker radiates a MLS signal from a horizontal distance *d* to the microphones, and a height *Hs*, (height of source). The parameters of a ground impedance model were modified and compared with the experimental curve. The difference in the impedance of the soil between the experimental and the theoretical curves is minimized [16].

The ANSI S1.18 Standard proposes three geometries: A, which covers a wider range of frequencies, B, which emphasizes the effect of the ground at frequencies above 1000 Hz, and is recommended for hard soils, and C which highlights the effect of the soil at frequencies below 1000 Hz, and should be used for soft grounds.

The ANSI S1.18 standard covers a frequency range of 250–4 kHz. It recommends using a signal with level at least 10 dB above the background noise level. In any case, you should use windscreens for microphones. The soil must be flat. We accomplished the recommendations of the standard.

Kruse and Mellert [17] recommended a slightly different geometry, obtained after an errors minimization process in the frequency range between 100 and 400 Hz. but in this case we use different geometry, obtained after a geometry optimization process in the frequency range between 0.3 and 7 kHz, due to the experimental conditions.

4.1. Measurements in movement at different speeds

For all the measurements along different avenues we used the following configuration, $Hs = 0.165$ m, $Ht = 0.165$ m, $Hb = 0.06$ m and $d = 0.4$ m. MLS signals of order 18 were used, with 3 averages, and sample frequency of $Fs = 96$ kHz. Fig. 4 shows the experimental setup and the ground patch of asphalt to perform the characterization. The source can be seen oriented in the direction of the support holding the two microphones. Firstly a measurement was made in a static position, then at different speeds 10–100 km/h. Fig. 5 shows the impulse responses of top and bottom microphones at different speeds, 20 km/h and 100 km/h, as can be seen the impulse response at 20 km/h has a higher amplitude, because the aerodynamic noise is lower than at 100 km/h, as well as the dynamic range. Fig. 6 shows the level difference curves measured at various speeds: 0, 20, 50 and 100 km/h. Fig. 6a shows that, as the speed increases, the resulting curve is contaminated with aerodynamic and background noises. Then, applying a temporal window to remove the unwanted reflections and the noise, the experimental difference curves can be seen clearly in Fig 6b.

Fig. 4. Experimental setup and contact path.

5. Experimental results

A MATLAB Graphical User Interface (GUI) was designed to acquire and to identify the characteristics of the ground surface measured according with a variant of the ANSI S1.18 standard. Its implementation allows selecting the values for the position of the source and receivers, and the atmospheric conditions. Impedance models are considered with a surface's configuration of homogeneous layers and with local reaction. The user interface allows plotting the level difference between the two sensors, the windowed original signal and a theoretical curve fitted to the experimental curve according to the geometrical set up, and values of one, two, three and four parameters as a result.

Fig. 7, shows the home window of the Graphical User Interface (GUI), which is a useful tool to facilitate the measurement and characterization of the ground surface and extract important parameters. The application is simple and functional, as it provides the necessary options to select from 1 to 4 of the parameters described previously, allowing the user to enter data regarding the location of the sound source and receivers, as the experimental curve needs to be compared with the theoretical curves in the same geometrical arrangement. For this experiment the following values were used; source height (Hs) = 0.165 m, height of top microphone (Ht) = 0.165 m, height of bottom microphone (Hb) = 0.06 m and distance between source and microphones (d) = 0.4 m. Weather conditions are also important, since the determination of sound propagation requires information on temperature, relative humidity and barometric pressure as a function of height near the propagation path. These values determine the sound speed profile. Ideally, the altitude at which the meteorological data are collected should reflect on the application. If this information is not available, then there are alternative procedures. It is possible,

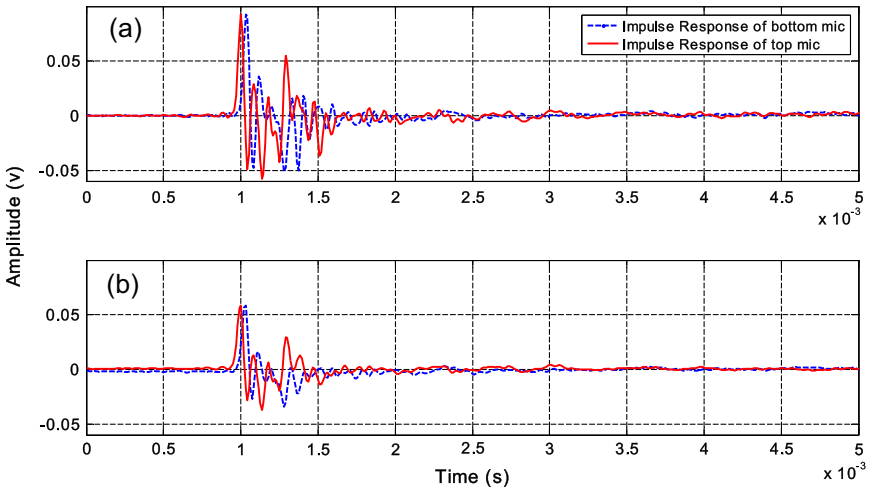

Fig. 5. Impulse responses at 20 km/h (a) and at 100 km/h (b).

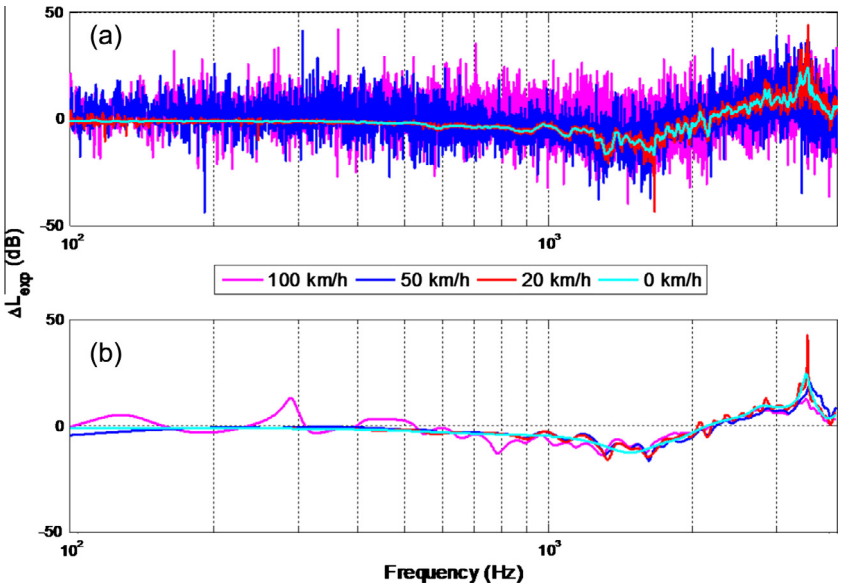

Fig. 6. Experimental difference curves at different speeds without a temporal window applied (a) and with temporal window applied (b).

for instance, to generate an approximate sound speed profile from temperature and wind speed at a given altitude using the similarity theory [18,19] and to input this directly. The atmospheric conditions in our experiments were: temperature $T = 24$ °C, atmospheric pressure $Pa = 1007$ mb and relative humidity $H = 30\%$, allowing us to obtain the air density ($\rho_0 = 1.17$ kg/m^3), sound speed in air ($C_0 = 345.5$ m/s) and air impedance ($Z_0 = 406.5$ N s/m^2). This will allow a more accurate estimation for specific conditions. In the right-hand part of Fig. 7, the impedance model can be selected, depending on how many parameters are required. For example one parameter: flow resistivity σ; two parameters: flow resistivity σ and layer thickness τ; two parameters: flow resistivity σ and rate of change of porosity α; three parameters: flow resistivity σ, porosity φ and tortuosity T; and four parameters: flow resistivity σ, porosity φ, tortuosity T and shape factor ζ. To start the measurement the acquisition data button is pressed and the results can be obtained in less than 5 s.

In order to make the comparison and adjustment between the experimental and theoretical curves, a code in Matlab was implemented, establishing all the ranges for each parameter under test, and a nonlinear programming that attempts to find a constrained minimum of a scalar function of several variables starting at an initial estimate [20]. This is generally referred to as constrained nonlinear optimization [21].

The following equation finds the minimum of a problem specified by

$$\min f(x) \text{ such that } \begin{cases} c(x) \leqslant 0 \\ ceq(x) = 0 \\ A \cdot x \leqslant b \\ Aeq \cdot x = beq \\ lb \leqslant x \leqslant ub, \end{cases} \tag{13}$$

x, b, beq, lb, and ub are vectors, A and Aeq are matrices, $c(x)$ and $ceq(x)$ are functions that return vectors, and $f(x)$ is a function that returns a scalar. $f(x)$, $c(x)$, and $ceq(x)$ can be nonlinear functions.

The frequency fitting range for comparing the theoretical curves, for this case is 1–5 kHz, due to the absorption and reflection in the path. In Fig. 8, the final result shows the 4 parameters, in the case of a speed of 20 km/h: $\sigma = 0.78 \times 10^6$ N s/m^4, $\varphi = 0.9$, $T = 1$ and

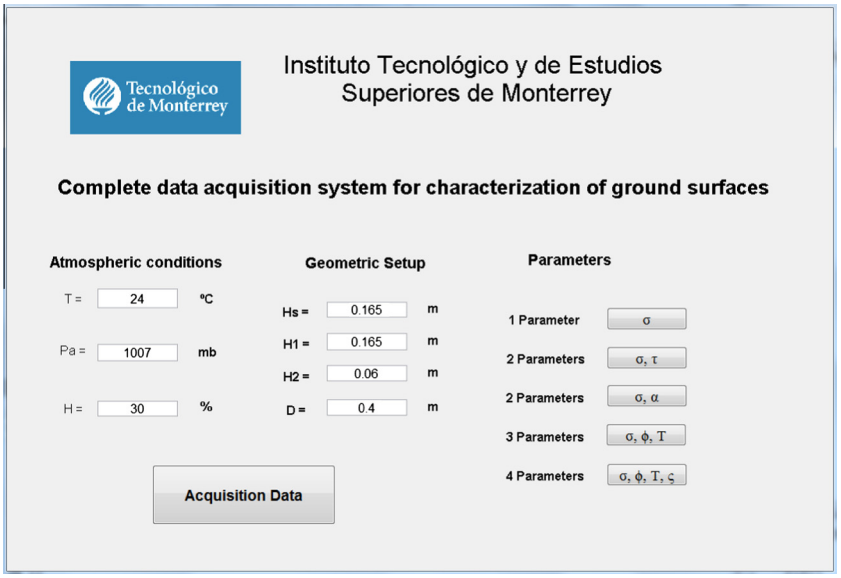

Fig. 7. Graphical user interface of data acquisition system.

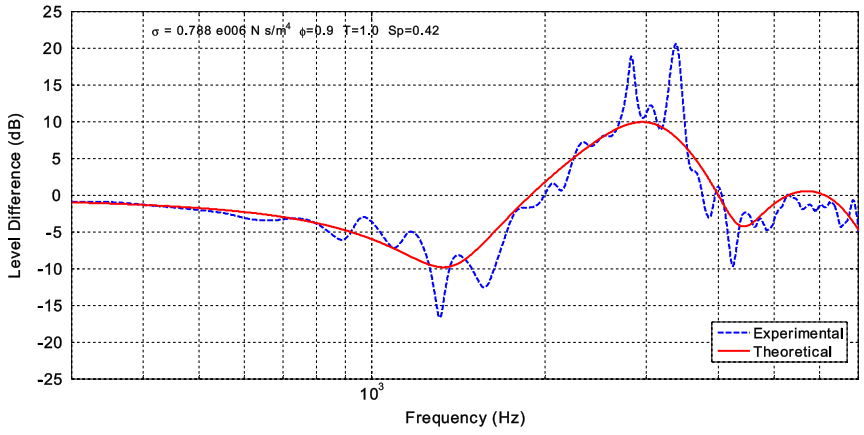

Fig. 8. Theoretical and experimental level difference curves for the asphalt at 20 km/h.

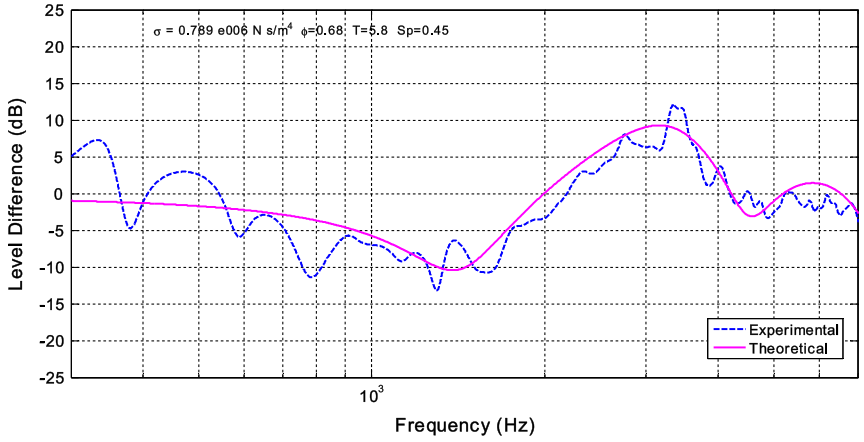

Fig. 9. Theoretical and experimental level difference curves for the asphalt at 100 km/h.

$\zeta = 0.42$; the result in the GUI plots the original signal windowed (blue) and the theoretical (red) curve, displaying minor discrepancies between them.

In all the cases we applied a temporary window in both signals (top and bottom microphones) so as to eliminate the unwanted reflections incoming from close obstacles and decrease the back-

Table 1
Four ground parameters obtained at different speeds.

Speed (km/h)	Flow resistivity ($N\,s/m^4 \times 10^6$)	Porosity	Tortuosity	Shape factor	Mean squared error	Absolute error
0	0.78	0.90	1.2	0.42	3.2	2.2
10	1.20	0.91	1.0	0.49	3.1	2.0
20	0.95	0.90	1.1	0.48	3.1	2.0
30	1.10	0.92	1.3	0.47	3.1	2.1
40	0.92	0.90	1.0	0.49	2.5	1.8
50	0.95	0.29	1.4	0.46	2.8	2.2
60	0.67	0.90	1.0	0.49	2.4	1.8
70	0.95	0.56	1.4	0.49	2.6	2.0
80	0.61	0.54	1.0	0.49	2.2	1.7
90	0.70	0.45	1.7	0.49	2.5	2.0
100	0.78	0.68	5.8	0.45	2.5	2.0

ground noise [22]. Fig. 9 shows another final result, using 4 parameters; in this case, a speed of 100 km/h, $\sigma = 0.78 \times 10^6$ N s/m^4, $\varphi = 0.68$, $T = 5.8$ and $\zeta = 0.45$. The result in the GUI plots the original signal windowed (blue) and the theoretical (pink) curve displaying minor differences between them.

Table 1 displays the 4 parameters obtained at different speeds, acquired along 10 km of some avenues. As can be seen, the 4 parameters are consistent and reasonable, with the flow resistivity parameter showing more variation, between 0.6–1.2 $\times 10^6$ N s/m^4. The other 3 parameters showed fewer discrepancies due to the characteristics of asphalt. In Table 1 also is shown the Mean Squared and the absolute Errors between the experimental and theoretical curves according to Zhang et al. [23,24].

6. Summary and conclusions

With an on-board data acquisition system we can obtain the parameters of ground surfaces in real time at different speeds. The system is based on two small microphones with flat response frequency, a small directional speaker, audio interface and a laptop for signal processing.

The contribution of this system is to know, in real time (less than 5 s, depends of processing speed), the physical parameters of ground surface measured at different speeds driving a car, minimizing the influence of aerodynamic noise. The low cost and its portability make the system to be a very useful tool for noise predictions in outdoors propagation and could be used as a complementation in noise mapping. Other potential application is the scouting of the rolling surface in order to adjust the brake and suspension system of smart vehicles [25].

Calculating the impedance of the ground surface requires a starting geometry and initial atmospheric conditions, which are important in the propagation of sound. We have presented a data acquisition system that facilitates the measurement and the identification of 4 parameters of the ground surface with a simple and interactive tool (GUI in Matlab). Besides plotting the level difference between the two sensors of the experimental signal, it also plots the theoretical curve according to the geometrical set up and the values of the parameters used: flow resistivity, porosity, tortuosity and shape factor.

In this work we have used a number of models to describe various types of grounds, starting from the simplest [2], using flow resistivity as the single parameter to describe the material, to more complex models that need a complete acoustic characterization of the surface [26]. Using these mathematical models, we have made a characterization of the road surface in real time, implemented in a portable optimized system. The measured and theoretical excess attenuation curves provide reasonable values of the 4 parameters showing a good agreement in all cases. Due to its low cost and its portability make the system to be a very useful and newfangled tool, in order to characterize a complete route as an instrument in noise mapping.

Acknowledgments

This work has been possible thanks to funding by CONACYT and ITESM.

References

[1] Morse PM, Ingard KU. Theoretical acoustics. New York: McGraw-Hill; 1968.
[2] Delany ME, Bazley EN. Acoustical properties of fibrous absorbent materials. Appl Acoust 1970;3:105–16.
[3] Garai M. Measurement of the absorption coefficient in situ: the reflection method using periodic pseudorandom sequences of maximum length. Appl Acoust 1993;39:119–39.
[4] Cobo P, Fernández A, Cuesta M. Measuring short impulse responses with inverse filtered maximum-length sequences. Appl Acoust 2007;68:820–30.
[5] Ortiz S, Kolbrek B, Cobo P, Gonzalez L, De la Colina C. Point source loudspeaker design: advances on the inverse horn approach. Audio Eng Soc 2014;62(5).
[6] Attenborough K. Sound propagation close to the ground. Annu Rev Fluid Mech 2002;34:51–82.
[7] Attenborough K, Li KM, Horosenkhov K. Predicting outdoor sound. London: Taylor & Francis; 2008.
[8] Xie H-S. On numerical calculation of the plasma dispersion function. IFTS-ZJU 2010.
[9] Mechel FP. Formulas of acoustics. Berlin: Springer Verlag; 2008.
[10] Ibarra D, Cobo P, Anfosso-Lédée F. Relationship between the noise radiated by a vehicle to the near and the far fields. Noise Cont Eng J 2013;61:446–57.
[11] NT ACOU 104. Ground surfaces: determination of the acoustic impedance. Finland: NORDTEST; 1999.
[12] Guillaume G, Faure O, Gauvreau B, Junker F, Berengier M, L'Hermite P. Estimation of impedance model input parameters from in situ measurements: principles and applications. Appl Acoust 2015;95:27–36.
[13] Ibarra D, Ramirez-Mendoza R, Lopez E, Bustamante R. Influence of the automotive Start/Stop system on noise emission: experimental study. Appl Acoust 2015;100:55–62.
[14] ANSI S1.18. Template method for ground impedance. American National Standards Institute, Acoustical Society of America; 1999.
[15] Attenborough K, Bashir I, Therzadeh S. Outdoor ground impedance models. J Acoust Soc Am 2011;129:2806–19.
[16] Bravo T, Ibarra D, Cobo P. Far-field extrapolation of maximum noise levels produced by individual vehicles. Appl Acoust 2013;74:1463–72.
[17] Kruse R, Mellert V. Effect and minimization of errors in situ ground impedance measurements. Appl Acoust 2008;69:884–90.
[18] Sutherland LC, Daigle GA. Atmospheric sound propagation. In: Crocker MJ, editor. Handbook of acoustics. New York: John Wiley & Sons; 1999.
[19] Shaffer SR, Fernando HJS, Ovenden NC, Moustaoui M, Mahalov A. Simulating meteorological profiles to study noise propagation from freeways. Appl Acoust 2015;92:102–14.
[20] Byrd RH, Gilbert JC, Nocedal J. A trust region method based on interior point techniques for nonlinear programming. Math Programm 2000;89(1):149–85.
[21] Coleman TF, Li Y. An interior, trust region approach for nonlinear minimization subject to bounds. SIAM J Opt 1996;6:418–45.
[22] Cobo P, Ortiz S, Ibarra D, de la Colina C. Point source equalised by inverse filtering for measuring ground impedance. Appl Acoust 2013;74:561–5.
[23] Tudon-Martinez J, Fergani S, Sename O, Martinez J, Morales-Menendez R, Dugard L. Adaptive roard profile estimation in semiactive car suspensions. IEEE Trans Control Syst Technol 2015:1063–6535.
[24] Zhang L, Gu T, Zhao J, Ji S, Hu M, Li X. An improved moving least squares method for curve and surface fitting. Math Prob Eng. 2013 [ID 159694].
[25] Zhang L, Gu T, Zhao J, Ji S, Sun Q, Hu M. An adaptive moving total least squares method for curve fitting. Measurement 2014;49:107–12.
[26] Lui WK, Li KM. A theoretical study for the propagation of rolling noise over a porous road pavement. J Acoust Soc Am 2004;116:313–22.